AEM Accepted Manuscript Posted Online 2 March 2018
Appl. Environ. Microbiol. doi:10.1128/AEM.01732-17

Plant homeodomain (PHD) genes play important roles in cryptococcal yeast-hypha transition

Running title: PHD genes regulate *Cryptococcus* morphotype transition

Yunfang Meng[1, 2, 3#], Yumeng Fan[2, 4#], Wanqing Liao[3*], and Xiaorong Lin[2, 4*]

[1]Department of Dermatology, Shandong Provincial Hospital Affiliated to Shandong University, Jinan 250021, China

[2]Department of Biology, Texas A&M University, College Station, Texas 77843, USA

[3] Department of Dermatology and Venereology, Changzheng Hospital, Shanghai 200003, China

[4] Department of Microbiology, University of Georgia, Athens, Georgia 30602, USA

[#] These authors contributed equally to this work.

* Correspondence:

Email: Xiaorong.Lin@uga.edu

liaowanqing@sohu.com

Abstract

Cryptococcus neoformans is a major opportunistic fungal pathogen. Like many dimorphic fungal pathogens, *C. neoformans* can undergo morphological transition from the yeast form to the hypha form and its morphotype is tightly linked to its virulence. Although some genetic factors controlling morphogenesis have been identified, little is known about the epigenetic regulation in this process. Proteins with the plant homeodomain (PHD) finger, a structurally conserved domain in eukaryotes, are first identified in plants and are known to be involved in reading and effecting chromatin modification. Here, we investigated the role of the PHD finger family genes in *Cryptococcus* mating and yeast-hypha transition. We found 16 PHD finger domains distributed among 15 genes in the *Cryptococcus* genome, with two genes, *ZNF1*α and *RUM1*α, located in the mating type locus. We deleted these 15 PHD genes and examined the impact of their disruption on cryptococcal morphogenesis. The deletion of five PHD finger genes dramatically affected filamentation. The *rum1*αΔ and the *znf1*αΔ mutants showed enhanced ability to initiate filamentation but impaired ability to maintain filamentous growth. The *bye1*Δ and the *phd11*Δ mutants exhibited enhanced filamentation, while the *set302*Δ mutants displayed reduced filamentation. Ectopic overexpression of these five genes in the corresponding null mutants partially or completely restored the defect in filamentation. Furthermore, we demonstrated that Phd11, a suppressor of filamentation, regulates the yeast-hypha transition through the known master regulator Znf2. The findings indicate the importance of epigenetic regulation in controlling dimorphic transition in *C. neoformans*.

Key words

plant homeodomain (PHD) finger, morphogenesis, pheromone, unisexual development, dimorphism

Importance

Morphotype is known to have profound impact on cryptococcal interaction with various hosts, including mammalian hosts. The yeast form of *Cryptococcus neoformans* is considered the virulent form while its hypha form is attenuated in mammalian models of cryptococcosis. Although some genetic regulators critical for cryptococcal morphogenesis have been identified, little is known about epigenetic regulation in this process. Given that plant homeodomain (PHD) finger proteins are involved in reading and effecting chromatin modification and their functions are unexplored in *C. neoformans*, we investigated the role of the 15 PHD finger genes in *Cryptococcus* mating and yeast-hypha transition. Five of them profoundly affect filamentation as either a suppressor or an activator. Phd11, a suppressor of filamentation, regulates this process *via* Znf2, a known master regulator of morphogenesis. Thus, epigenetic regulation, coupled with genetic regulation, controls this yeast-hypha transition event.

1. Introduction

Cryptococcus neoformans is an opportunistic fungal pathogen that claimed hundreds of thousands of lives each year globally (1, 2). This fungus can undergo morphological transition from the yeast form to the hypha form. Like many dimorphic fungal pathogens (3, 4), morphotype of *Cryptococcus* is tightly linked to its virulence (5, 6). To understand the biology and pathology of *Cryptococcus*, some important genetic factors that regulate yeast-hypha transition have been identified. Morphological transition in *Cryptococcus* occurs during unisexual development or during bisexual **a**-α mating (7-9), which is controlled by the pheromone signaling pathway under mating-inducing conditions (10). The HMG domain transcription factor Mat2 is an effector of the pheromone pathway (11). Mat2 activates the zinc finger transcription factor Znf2 under mating-inducing conditions, which ultimately determines the yeast-hypha transition (11). Znf2 is the decision maker of filamentation, and it also bridges morphology and virulence potential in *Cryptococcus* (6, 11, 12).

The mating-type locus of *Cryptococcus* genome carries many genes that control the mating process (13), including several components of the pheromone pathway such as the pheromone gene *MF*α/**a** (14, 15), the pheromone receptor gene *STE3*α/**a** (14, 16), *STE20*α/**a**, and elements of MAPK cascade *STE11*α/**a** and *STE12*α/**a** (9, 17). The mating type locus also harbors the cell identity factor *SXI1*α/2**a** (13, 18). Two uncharacterized plant homeodomain (PHD) finger genes, *RUM1* α/**a** and *ZNF1* α/**a**, are also located in the mating-type locus (13, 15). PHD finger was first identified in plant *Arabidopsis* (19). The highly conserved small PHD fold consists of 50-80 amino acid residues and a cross-brace topology in which two zinc atoms anchored by the Cys4-His-Cys3 motif. PHD finger proteins are important readers of histone modifications and are involved in epigenetic regulation in plants and mammals (20). Although PHD finger proteins

are universally distributed in eukaryotes, their biological function in the fungal kingdom is poorly understood. In another human fungal pathogen *Candida albicans*, histone modification contributes to its yeast-hypha transition (21), indicating that epigenetic factors can be important in regulating fungal morphogenesis. However, nothing is known about epigenetic regulation of morphogenesis in *Cryptococcus*.

Here, we systematically analyzed the PHD finger genes in the genome of *C. neoformans*. We identified 16 PHD finger domains harbored by 15 genes. We generated and characterized 15 PHD gene knockout mutants and five PHD gene overexpression strains. These five selected PHD genes exhibit important roles in filamentation, indicating that some PHD proteins are critical for *Cryptococcus* morphotype transition.

2. Results

2.1 Identification of PHD finger genes in *Cryptococcus neoformans*

As mentioned earlier in the introduction, two PHD finger genes *RUM1* and *ZNF1* are located in the mating type locus. To identify additional putative PHD finger-containing genes, we used the PHD domain sequences from *ZNF1*α as the query sequences to BLAST search against the genome of the *C. neoformans* strain JEC21 (serotype D). Based on the Pfam database, we obtained 16 putative PHD finger domains carried by 15 genes in the genome of JEC21 (Table 1). The corresponding genes also exist in the genome of the *C. neoformans* strain H99 (serotype A). Predicted protein sequences of these PHD genes were compared with PHD proteins in other eukaryotic species, including budding yeast, fission yeast, mouse, and human. However, these homologous are not conserved with cryptococcal PHD genes except some conserved domains.

The closest homologs of some PHD proteins in *Saccharomyces cerevisiae* that have been previously characterized are provided in Table 1.

Alignment of these PHD finger domain sequences by the DNAMAN software indicated that they share a feature with the same basic PHD finger topology: two zinc atoms harbored by the Cys4-His-Cys3 motif (Figure 1A), as expected based on previous studies (20). The motif scan results revealed additional important domains related to histone modification in Phd11 and Set302 (Figure 1B). Phd11 carries a MOZ-SAS domain, which may potentially possess the lysine acetyltransferase activity (22). Set302 harbors one SET domain, which shows histone methyltransferase activity in *S. cerevisiae* and other organisms (23, 24). The homologue in *Saccharomyces* forms a Set3 complex, which acts as a meiotic-specific repressor of the sporulation genetic program (23). The presence of these motifs in Phd11 and Set302 in *Cryptococcus* suggests that these PHD proteins might act as chromatin modifiers in addition to chromatin readers.

2.2 Different expression patterns of the PHD genes during development

XL280 has been widely used as a reference strain to study morphogenesis, sexual development, and pathogenicity (12, 25-28). It has superior ability to transit from the yeast form to the hypha form (29, 30). We decided to examine if PHD genes are involved in cryptococcal development in the wild-type XL280 strain during vegetative yeast growth in YPD medium and during unisexual development on V8 juice agar medium (31, 32). We first examined their expression pattern by RNA-Seq and real-time PCR.

When the wild-type cells were cultured in YPD medium, the transcript levels of the PHD finger genes were 2^5 to 2^9 fold lower than the house keeping gene *TEF1* (translation elongation factor 1) based on our previous RNA-Seq data (33) (Figure 2A). The real-time PCR results of the wild-type strain XL280 cultured in YPD liquid medium for 16 hours were largely consistent with the pattern observed through the RNA-Seq data (Figure 2B). The low transcript levels of the PHD finger genes compared to the house-keeping gene *TEF1* are consistent with their potential regulatory roles.

Many morphogenesis factors show development-associated transcription. To examine if the transcript levels of the PHD finger genes change at different cryptococcal development stages under a mating-inducing condition, we analyzed the FPKM values of the PHD genes from our RNA-Seq data obtained from wild-type XL280 cultured alone on YPD medium (yeast growth) and on V8 medium for 24 hours (initiation of filamentation), 48 hours (filamentation elongation), or 72 hours (filamentation and initiation of sporulation). Interestingly, although the transcript levels of PHD finger genes remained low under all the conditions tested, the transcript levels of *BYE1*, *PHD4*, *PHD5*, *PHD11*, *SET302*, *ZNF1*α, and *PHD15* dramatically increased after 24 h to 72 h culture on V8 medium compared to those in YPD medium, particularly at the later time points (Figure 3). The transcript level of *PHD6* and *PHD9* only showed significant increase at the 72 h time point.

We also tested the transcription levels of PHD genes during α-**a** bisexual mating on V8 medium. Here, we co-cultured XL280α and its congenic pair strain XL280**a** (12) on V8 medium for bisexual mating. We found that the transcript levels of *BYE1*, *PHD4*, *PHD6*, *PHD11*, *SET302* and *PHD16* genes were increased more than 4 fold after 24 h or 48 h during bisexual mating on V8 medium compared to those in YPD (Figure 4). The observations suggest that the

139 expression of the PHD family genes in *C. neoformans* is positively correlated with the
140 filamentation process. In particular, the transcript level of *PHD4* during bisexual mating on V8
141 medium was dramatically increased compared to that in YPD medium, with the maximum of
142 120 fold increase at the 48 hour time point (Figure 4). Together, both RNA-Seq and real-time
143 PCR data suggest that PHD genes, particularly *BYE1*, *PHD4*, *PHD6*, *PHD11*,and *SET302* may
144 play a role in cryptococcal development based on their development-associated expression.

145

146 2.3 Phenotypical characterization of the PHD gene deletion mutants

147 To characterize the biological roles of the PHD genes, we deleted the 15 PHD finger
148 genes individually in the XL280 background. Given that *C. neoformans* is a fungal pathogen
149 with well-established virulence traits, we first examined if the deletion of these genes would
150 affect the following traits: thermo-tolerance, UV-sensitivity, capsule production, and
151 melanization. Many fungal species cannot tolerate or grow at the mammalian body temperature
152 (34), a perquisite for systemic infections. Consequently, temperature-sensitive cryptococcal
153 mutants such as calcineurin mutants or RAM pathway mutants are often avirulent (35-37). Most
154 of the PHD gene deletion mutants grew well at 30°C, 37°C, or 39°C, similar to the wild type
155 (Figure 5A). The *bye1*Δ mutant showed modest growth reduction at 37°C, while the *phd3*Δ and
156 the *phd15*Δ mutants showed severe growth defect at both 30°C and 37°C (Figure 5A). Colonies
157 of the *phd3*Δ and the *phd15*Δ mutants were smaller compared to those of the wild type even at
158 30°C, and their growth defects appeared to be much more severe at higher temperatures. At 39°C,
159 there was barely any growth observed in the *phd3*Δ mutant or the *phd15*Δ mutant, and some
160 growth was recovered after temperature downshift from 39°C to 30°C (Figure 5B). To determine

161 if the smaller colony size is due to a slower growth rate or a smaller cell size at 30°C, we
162 examined the generation time of the *phd3*Δ mutant and its cell size. We did not observe any
163 significant difference in cell size in the *phd3*Δ mutant compared to the wild type (Figure 5C). As
164 expected, the generation time for the *phd3*Δ mutant was twice as long compared to the wild type
165 at 30°C in YPD liquid culture (Figure 5D). We also tested the sensitivity of all the PHD finger
166 deletion mutants to UV radiation. Most were similarly sensitive to the UV radiation as the WT
167 strain (Figure 6A) with the exception of the *phd3*Δ mutant, which showed increased resistance
168 (Figure 6A-B). Interestingly, the other slow-growing *phd15*Δ mutant did not show significant
169 increased resistance to UV radiation, suggesting that Phd3 and Phd15 are not functionally
170 identical. Melanin and capsule production are two other major virulence traits for *Cryptococcus*.
171 All mutants were capable of producing melanin on the L-Dopa medium (Supplemental Figure
172 1A), and all formed capsule with no apparent defects based on microscopic examination using
173 Indian ink negative staining (Supplemental Figure 1B). Thus, it appears that most of the PHD
174 genes are not critical for expressing these classic virulence traits.

175

176 ## 2.4 Five PHD genes are important for yeast-hyphal transition.

177 Besides the classic virulence traits, morphotype has a profound impact on cryptococcal
178 interactions with various hosts. Filamentation confers *Cryptococcus* resistance to predation by
179 soil amoeba (38), but filaments are immune-stimulatory in mouse model of cryptococcosis (5,
180 39). As PHD domain proteins are known to be involved in development in plants and animals
181 (20, 40, 41), we decided to examine their role in morphogenesis and sexual development in
182 *Cryptococcus*. *C. neoformans* undergoes bisexual mating involving α and **a** cells (no mating type
183 switch) (7, 42), and it can also undergo unisexual development that involves cells of only one

184 mating type (43). During unisexual development, colonies derived from a single cell (and thus a
185 single mating type) can filament and generate meiotic progeny (25, 27, 28, 43).

186 We first examined these PHD gene deletion mutants for self-filamentation during
187 unisexual development at 48 hours and 96 hours after inoculation on V8 medium. Filamentation
188 in wild-type XL280 became obvious under stereoscope at 48 hours post inoculation and
189 filaments were clearly visible as the white fluffy edge of the colony at 96 hours post inoculation
190 (Figure 7). Among the 15 mutants, five mutants namely *bye1*Δ, *phd11*Δ, *set302*Δ, *rum1*αΔ, and
191 *znf1*αΔ displayed alteration in filamentation (Figure 7). Reduction in filamentation was also
192 observed in the *phd3*Δ and *phd15*Δ mutants. However, given their growth defects and
193 temperature-sensitive phenotype (Figure 5), we decided not to focus on these two mutants. The
194 *bye1*Δ and *phd11*Δ mutants showed more robust hyphal growth than the wild type both at 48
195 hours and at 96 hours post inoculation (Figure 7A-B), indicating that Bye1 and Phd11 normally
196 repress filamentation. In contrast, the *set302*Δ mutant exhibited drastically reduced filamentation
197 at both time points examined (Figure 7A-B), suggesting that Set302 is an activator for
198 filamentation. Interestingly, the *rum1*αΔ and the *znf1*αΔ mutants showed slightly increased
199 robustness in filamentation at 48 hours, but ended up with shorter filaments than the wild type at
200 96 hours (Figure 7A-B). This suggests that Rum1 and Znf1 repress the initiation of filamentation
201 but they are required for sustained hyphal growth.

202 Filamentation proceeds sporulation in *Cryptococcus*. To examine if these five PHD genes
203 that regulate filamentation also play a role in sporulation, we examined the corresponding gene
204 deletion mutants for their ability to sporulate. The wild-type strain produced basidia with four
205 long chains of spores after one week of incubation on V8 medium (Supplemental Figure 2). The
206 *set302*Δ mutant rarely yielded spore chains at this point, but eventually produced spores after

prolonged incubation. This delay in sporulation was likely due to its severely impaired hyphal growth (Figure 7A-B). All other mutants were able to produce normal and abundant spore chains (Supplemental Figure 2). This result demonstrates that PHD genes were not specifically required for sporulation.

Based on the results obtained with the gene deletion mutants, five PHD genes, namely *BYE1*, *PHD11*, *SET302*, *RUM1*α and *ZNF1*α, play important roles in regulating filamentation. To further examine their roles in filamentation, we decided to constitutively express these PHD genes using the promoter of the house-keeping gene *GPD1*. For Phd11, we also fused the fluorescence protein mCherry in frame to its C-terminus. We then introduced these PHD gene overexpression constructs ectopically into the corresponding gene deletion mutants. Increased transcript levels of these PHD genes in the transformants were observed based on the real-time PCR results (Supplemental Figure 3), indicating that these strains indeed overexpress the corresponding PHD genes compared to the wild type. We then examined self-filamentation of these strains. We found that overexpression of *SET302*, *RUM1*α, and *ZNF1*α led to complete or partial restoration in filamentation in the corresponding *set302*Δ, *rum1*αΔ, and *znf1*αΔ mutants (Figure 7C). Interestingly, overexpression of *BYE1* and *PHD11* suppressed the overly robust filamentation of the *bye1*Δ and *phd11*Δ mutants (Figure 7C), corroborating their roles as repressors for filamentation. Collectively, our data indicate that these five PHD genes play important roles in controlling filamentation. The phenotypes of the gene deletion mutants and the gene overexpression strains indicate that Bye1 and Phd11 suppress filamentation while Set302 enhances filamentation. Rum1 and Znf1 suppress the initiation of filamentation but they are important to sustain filamentous growth.

2.5 The impact on the pheromone and the filamentation genes caused by changes of the PHD finger genes.

The evidence presented above reveals the importance of the five PHD genes in regulating filamentation. As mentioned in the introduction, the pheromone pathway is a well-characterized pathway that activates filamentation in *Cryptococcus* under mating-inducing conditions. The transcription factor Mat2 is essential in controlling this pheromone sensing and response pathway and is required for cell fusion (11). Mat2 then activates Znf2 under mating-inducing conditions (6, 11). Znf2 is the key transcription factor that is required for filamentation under all conditions tested. Deletion of *ZNF2* itself does not abolish the pheromone pathway or cell fusion (11). Since the disruption of the PHD finger genes altered filamentation, we speculate that these PHD finger genes may directly or indirectly affect Znf2 *via* pheromone-dependent or pheromone-independent pathways.

If a mutant cannot sense or response to pheromone, cell fusion will be abolished, as we observed previously for the *mat2*Δ mutant (11). To determine if any of the five PHD finger proteins are essential for cell fusion, the gene deletion mutants in the XL280α background (G418-resistant or NAT-resistant) were co-cultured with the wild-type **a** mating partner carrying a different drug-selection marker on V8 medium. Cell fusion products with two different drug-resistance markers were easily recovered from all crosses between the PHD deletion mutants (α) and the wild-type **a** mating partner. By contrast, no fusion products were recovered when the *mat2*Δ mutant was co-cultured with a compatible wild-type mating partner, consistent with the essential role of Mat2 in cell fusion. The ability of the PHD mutants to undergo bisexual mating is also supported by the fact that we obtained all the PHD mutants in the mating type **a** background by crossing the mutants in the α mating type with XL280**a** (Table 2). The results

253 indicate that these PHD genes, unlike genes in the pheromone pathway, are not essential for cell
254 fusion.

255 We further examined the effect of the disruption or overexpression of these PHD genes
256 on the expression of the pheromone pathway controlled by Mat2 and the filamentation pathway
257 controlled by Znf2. Here we chose to measure the transcript level of *MF*α and *CFL1*, the
258 respective downstream factor of Mat2 and Znf2. It is known that their transcript levels reflect the
259 activity of these two transcription factors (6, 11, 30). All the transcript levels in the mutants and
260 the wild-type control were normalized to that of the wild type cultured in YPD medium (Figure 8
261 & Supplemental Figure 4).

262 Cfl1 is a hypha-specific protein downstream of Znf2 and the transcript level of *CFL1*
263 correlates with filamentation (6, 11, 12, 44). In the *bye1*Δ mutant, the transcript level of *CFL1*
264 was approximately 16 fold higher than that of the wild type (Figure 8B), consistent with the
265 enhanced filamentation of the *bye1*Δ mutant (Figure 7A-B). In the $BYE1^{oe}$ strain, the pattern was
266 reversed and the transcript level of *CFL1* was more than 16 fold lower than that of the wild type
267 (Figure 8E). This is consistent with the decreased filamentation observed in the $BYE1^{oe}$ strain
268 (Figure 7C). Similarly, a higher *CFL1* transcript level (~ 2^5 fold) at 16 h time point was observed
269 in the *phd11*Δ mutant (Figure 8A), consistent with the enhanced filamentation of this mutant
270 (Figure 7A-B). Again, the pattern was reversed with a much lower *CFL1* transcript level (> 8
271 fold reduction) in the $PHD11^{oe}$ strain (Figure 7D), consistent with the reduced filamentation of
272 the $PHD11^{oe}$ strain (Figure 7C). The *rum1*αΔ and the *znf1*αΔ mutants showed increased
273 transcript level of *CFL1* (about 4-8 fold) at the 16 h time point. However, their *CFL1* transcript
274 level became comparable to that of the wild type at the 24 h time point. This is consistent with
275 our speculation that Rum1 and Znf1 suppress the initiation of hyphal growth but they are needed

to sustain filamentous growth. The *CFL1* transcript level was about 4 fold lower in the *set302*Δ mutant than that of the wild type at 24 h time point (Figure 8B), consistent with its reduced filamentation (Figure 7A-B). Surprisingly, the *CFL1* transcript level in the *SET302*^{oe} strain was still about 4-6 fold lower than that of the wild type even the strain showed robust hyphae growth. Overall, the transcript levels of *CFL1* in the PHD gene deletion and gene overexpression strains are largely consistent with their impact on filamentation.

In contrast to *CFL1*, the *MF*α transcript level in these PHD gene deletion and overexpression strains was not as predictable. For example, the *set302*Δ and the *bye1*Δ mutants showed opposite phenotype in term of filamentation, but their *MF*α transcript levels were similar. In *BYE1*^{oe} strain, the *MF*α level decreased dramatically (~ 2^5 fold changes) at 16 h and 24 h time points compared to that of the wild type. In the *rum1*αΔ and the *znf1*αΔ mutant, the *MF*α transcript levels were comparable with that of the wild type, while the transcript level of *MF*α in the *rum1*αΔ mutant only showed about 2 fold reduction at 24 h time point. The transcript levels of *MF*α were significantly different in the *phd11*Δ and the *PHD11*^{oe} strains at the 16 h time point (Supplemental Figure 4) and the difference became smaller at the later time point. The inconsistency of the *MF*α transcript levels in these strains with the mutant phenotype in filamentation is consistent with the idea that the pheromone pathway is not the major effector of these PHD proteins.

2.6 Phd11 functions upstream of Znf2 in regulating filamentation.

Although Znf2 is well-established for its essential role for hyphal growth (6, 11, 12), the regulatory circuits controlling Znf2, especially factors that suppress filamentation are unclear.

298 Given the phenotype of the *PHD11* gene deletion mutant (enhanced filamentation) and the
299 overexpression strain (reduced filamentation) (Figure 7A-C), Phd11 works as a suppressor for
300 filamentation. Here, we decided to further investigate the relationship between Phd11 and Znf2.
301 First, we examined the impact of deletion and overexpression of *ZNF2* on the transcript level of
302 *PHD11*. As shown in Figure 9A, the *PHD11* transcript levels in the wild-type strain, the *znf2*Δ
303 mutant, and the *ZNF2*^{oe} strain were similar regardless whether cells were cultured in YPD or on
304 V8 medium. This suggests that Znf2 does not affect Phd11 at the transcript level. We then
305 examined the transcript level of *ZNF2* in the wild type, the *phd11*Δ mutant, and the *PHD11*^{oe}
306 strain. As expected, the transcript level of *ZNF2* was low when wild-type cells were cultured in
307 YPD and it was drastically increased (~2^5 fold higher) when the wild-type cells were cultured on
308 V8 medium (Figure 9B). Although the deletion of *PHD11* did not show much impact on the
309 *ZNF2* transcript level, the overexpression of *PHD11* led to drastically reduced transcript level of
310 *ZNF2* (>2^6 fold reduction) on V8 medium when *ZNF2* is normally induced in the wild type.
311 Taken together, Phd11 may act upstream of Znf2 and negatively affect the *ZNF2* transcriptional
312 level.

313 To further investigate the relationship between *PHD11* and *ZNF2*, we made the
314 *phd11*Δ*znf2*Δ double mutant. The *phd11*Δ single mutant showed enhanced filamentation while
315 the *znf2*Δ single mutant was abolished in filamentation (Figure 9C). The *phd11*Δ*znf2*Δ double
316 mutant showed no hyphal growth, similar to the *znf2*Δ single mutant (Figure 9C). Thus, the
317 deletion of *PHD11*, although increased filamentation in a wild-type background, failed to confer
318 filamentation to the *znf2*Δ mutant.

319 To further examine the relationship between Phd11 and Znf2, we constructed a strain
320 with constitutive overexpression of *PHD11* and inducible expression of *ZNF2*. We hypothesize

that if Phd11 functions upstream of Znf2, then overexpression of *PHD11* when *ZNF2* is not expressed will recapitulate the *znf2*Δ-like non-filamentous phenotype. On the other hand, overexpression of the downstream factor *ZNF2* should overcome the suppressive effect by the overexpression of *PHD11* and drive robust filamentation. For this purpose, we had *PHD11* driven by the constitutively active *GPD1* promoter and *ZNF2* by the inducible promoter of the copper transporter gene *CTR4* (Figure 9D). Because V8 medium itself is slightly copper-limiting, the *CTR4* promoter will be activated under this condition and consequently *ZNF2* will be expressed. Indeed, the P_{CTR4}-*ZNF2*/*znf2*Δ strain showed robust hyphal growth on V8 medium (Figure 9E). The addition of copper to V8 medium will suppress the *CTR4* promoter and *ZNF2* will not be expressed. Consistently, the P_{CTR4}-*ZNF2*/*znf2*Δ strain grew only yeast colony in the presence of copper (Figure 9E). When *PHD11* was constitutively overexpressed, the strain P_{GPD1}-*PHD11*/*phd11*Δ showed repressed hyphal growth compared to the wild type (Figure 9E). When both *PHD11* and *ZNF2* were expressed on V8 medium, the strain P_{GPD1}-*PHD11*/P_{CTR4}-*ZNF2*/*znf2*Δ showed robust hyphal growth, similar to the $ZNF2^{oe}$ strain (Figure 9E). When excessive copper ion was added to the V8 medium, the expression of *ZNF2* was suppressed. This resulted in the non-filamentous phenotype of the strain P_{GPD1}-*PHD11*/P_{CTR4}-*ZNF2*/*znf2*Δ (Figure 9E), as we predicted. These results again corroborate the essential role of Znf2 in filamentation and demonstrate that Phd11 indeed functions upstream of Znf2 in controlling the yeast-to-hyphal morphological change.

3 Discussion

The plant homeodomain (PHD) finger is found in many chromatin-remodeling proteins in eukaryotes (20, 40, 41), and their activities could lead to altered gene expression and consequently regulate various biological processes. In our study, we systematically deleted PHD

finger genes in the environmental opportunistic fungal pathogen *Cryptococcus neoformans*. We found that *PHD3* and *PHD15* are critical for thermo-tolerance. Given that growth at mammalian temperature is a perquisite for cryptococcal pathogenesis, it would be interesting to identify their effector genes and investigate their potential impact on cryptococcal virulence in the future. Interestingly, we identified five PHD genes, namely *BYE1*, *PHD11*, *SET302*, *RUM1*, and *ZNF1*, that contribute to the yeast-hyphal morphological switch in *Cryptococcus*. Accordingly, we found that the deletion or overexpression of these five PHD genes alters the expression of filamentation-related genes. Among these five PHD finger genes, Bye1 and Phd11 work as suppressors of filamentation and Set302 functions as an activator of filamentation. Rum1 and Znf1, two PHD proteins encoded in the *MAT* locus, suppress the initiation of filamentation, but are important for maintaining robust hyphal growth. We chose to investigate Set302 and Phd11 further because *set302*Δ and *phd11*Δ showed the most dramatic and opposing phenotypes in terms of filamentation. Set302 and Phd11 are predicted to be nuclear proteins due to the presence of a nuclear localization signal (NLS). While attempts to construct mCherry-fused Set302 failed, the generated Phd11-mCherry indeed yielded stable and clear fluorescence that co-localized with the DAPI staining (Figure 10). The nuclear localization of Phd11 is consistent with its predicted nuclear function as a chromatin reader. Phd11 harbors a predicted histone acetyltransferase MOZ-SAS domain while Set302 contains a SET domain. The unique domain structures in these two PHD proteins suggest that Phd11 and Set302 may act not only as readers of histone modifications due to their PHD domains, but also as writers of histone modifications. Further mechanistic studies are warranted to fully understand their modes of action.

Materials and Methods

Strains and growth conditions

Strains used in this study are listed in Supplemental Table 1. All strains were stored as glycerol stocks at -80°C. For experiments, cells were streaked out from freezer stocks and cultured on YPD medium at 30°C (1% yeast extract, 2% Bacto Peptone, and 2% dextrose) unless indicated otherwise.

Construction of gene deletion mutants and overexpression strains

For gene deletion, we used the method of double-joint PCR as described previously (45). Briefly, two partially overlapping parts of the chosen drug selection marker (NEO, NAT, or HYG) were fused with the 5' or the 3' flanking regions (1 kb) of the open reading frame of each gene of interest respectively. The mixture of the pair of the fusion products were then introduced into the recipient strain by biolistic transformation as described previously (46). Transformants grown on the drug selective medium (YPD+NAT, YPD+NEO, or YPD+HYG) were checked for stability and stable transformants were then screened for homologous replacement events based on diagnostic PCR as described previously (47). Primers used in generating gene knockout strains and for screening the homologous replacement events are listed in the Supplemental Table 2. For gene overexpression, the ORF of the gene of interest was amplified using the genomic DNA of the wild-type strain XL280 as the template. The resulting amplicons were digested with restriction enzymes *Fse*I and *Pac*I and the digested products were then inserted into the plasmid pXL1 after the *GPD1* promoter as described previously (6). The resulting plasmids were linearized after restriction enzyme digestion and then introduced into *C. neoformans* cells by biolistic transformation as described previously (46) .Transformants grown on the drug selective medium (YPD+NAT, YPD+NEO, or YPD+HYG) were examined for stability after 5 passages on non-selective medium and the stable transformants were confirmed

by phenotypical assay, diagnostic PCR, or real-time PCR. For the inducible expression system, the construct was generated by the same method except that the amplicon was inserted after the *CTR4* promoter as described previously (6).

Construction of mCherry fused Phd11

The *PHD11* ORF was digested with restriction enzyme *FseI* and *AsisI* and then was introduced into the plasmid pXL1-mCherry between the *GPD1* promoter and mCherry in frame (6). Linearized plasmids were introduced into the corresponding *phd11*Δ mutant by biolistic transformation. Stable transformants were examined for the presence of mCherry fluorescence and for the increased transcript level of *PHD11* by real-time PCR. To examine the sub-cellular localization of Phd11-mCherry, the strain was cultured in liquid YPD at 30°C overnight. Cells were fixed with formaldehyde and stained with or without DAPI as described previously (48). Images were acquired using a Zeiss Imager M2 with an Axiocam 506 camera through the software Zen 11 (Carl Zeiss Microscopy). The mCherry signal was visualized using the filter FL filter set 43 HE Cy3 (Carl Zeiss Microscopy).

Mating and isolation of recombinant progeny

For the self-filamentation assay, the strains were first cultured in YPD liquid medium overnight. Cells were collected, washed with water, and resuspended to achieve the cell density of OD_{600}= 3.0. Then 5 microliters of the cell suspension were spotted onto V8 juice agar (5% V8 juice, 0.5 g/liter KH_2PO_4, 4% agar, pH=7) and cells were incubated at 22°C in the dark for the indicated period of time before images of the colonies were taken. For overexpression strains driven by the copper-inducible promoter, cell were maintained and cultured in YPD+200μM BCS, washed, and resuspended to achieve the cell density of OD_{600}=3.0. The cells were

412 inoculated onto V8 or V8+50μM BCS agar and then incubated as we described earlier. The
413 filamentation and the fruiting structure produced by unisexual development of each mutant were
414 examined under Olymbus CX41 microscope with a 20X objective after 2 weeks.

415 For bisexual mating, the α and **a** mating pair of the equal cell number were mixed and co-
416 cultured on V8 juice agar at 22°C in the dark. Bisexual mating was monitored by examining the
417 production of mating hyphae and spores microscopically. Spores were isolated by micro-
418 dissection. The genotype of the gene of interest (deletion or overexpression) of the dissected
419 progeny was confirmed by diagnostic PCR and by the presence or absence of the selective drug
420 marker. The mating type of the dissected progeny was determined by their ability to mate with
421 reference strains JEC21α and JEC20**a** as we described previously (12). Mendelian segregation of
422 the mating type and the drug marker (gene deletion) was confirmed prior to their usage in the
423 subsequent phenotypical analyses.

424 **Cell fusion assays**

425 Cell fusion assays were performed as previously reported (6, 11). Strains were first
426 cultured on YPD solid media for 2 days. Cells were collected and resuspended in water. Cell
427 concentration was measured by spectrophotometer at OD600 and adjusted to 3.00. Equal amount
428 of mating partner cells were mixed and 5 μl of the mixture were dropped onto V8 juice agar
429 medium (pH=7.0). The *bye1*Δ α mutant and the control wild-type XL280α with the G418
430 resistance marker (XL1348) were co-cultured with the wild-type mating parter JEC20**a** marked
431 with NAT^r (XL1142). Similarly, the *phd11*Δ α, *set302*Δ α, *rum1α*Δ, *znf1α*Δ, and the wild-type
432 XL280α with NAT resistance marker (XL1109) were co-cultured with the wild-type mating
433 partner JEC20**a** marked with $G418^r$ (XL1411). XL942α (*mat2::NAT*^{r}) and XL574α (*znf2::NAT*^{r})
434 co-cultured with JEC20**a** marked with $G418^r$ (XL1411) were used as the negative and positive

controls. After 16-hour of incubation at 22°C in the dark, colonies were cut off from plates and suspended in 1ml water. After 45 seconds vortex, cells were plated on YPD selective medium with NAT and G418 drugs and examined for the growth of the fusion products after 2 days of incubation.

In vitro phenotypic assays

In vitro phenotypic assays were performed as reported previously (49, 50). Briefly, cryptococcal strains were cultured in YPD liquid medium at 30℃ with shaking overnight and then washed twice with sterile water. All strains were adjusted to the same cell optical density (OD_{600}=3) and then 10X serially diluted. Then the serial dilutions of each strain (4 μl) were spotted onto various agar media for phenotypical analyses as described previously (51). To test the melanin production, yeast cells were spotted onto L-DOPA medium and incubated at 30℃ and 37℃ respectively. To characterize the production of capsule, cells were spotted onto RPMI medium and incubated at 37℃ with or without 5% CO_2. Capsule was visualized microscopically as a halo surrounding the yeast cell by India ink exclusion. For the temperature sensitivity test, yeast cells were spotted onto YPD medium and incubated at 30℃, 37℃, or 39℃ respectively. For the test for susceptibility to UV radiation, cells of different strains at the same concentration were spotted onto YNB agar medium and air-dried. Then the cells were exposed to 300J/m2 UV radiation for 0s, 3s, and 5s in a UV cross-linker. The treated cells were incubated at 30℃ for additional 2-3 days before the images of the colonies were taken.

Growth curve and generation time

The *phd3*Δ mutant and wild-type cells were inoculated in YPD liquid medium at the same cell density. Cultures were incubated at 30℃ with shaking at 225 rpm. Measurements at

457 OD_{600} with a spectrophotometer (SmartSpec Plus, BioRad) were taken at 1h intervals. The
458 experiment was carried out with three independent biological replicates. Data analysis was
459 performed with the Graphpad software.

460 **RNA purification and qPCR analyses**

461 Strains were cultured in YPD liquid medium at 30℃ overnight and washed twice with
462 distilled water. To examine the transcript levels during bisexual mating, equal number of cells
463 from the wild-type mating pair XL280α and XL280**a** (OD_{600}=1) were mixed and spotted onto V8
464 juice agar medium. Cells were incubated at 22°C in the dark. Cells from the co-culture were
465 collected from V8 medium at 0 h, 3 h, 10 h, 24 h, 48 h, and 72 h after incubation. The 0 hour
466 time point was used as the reference. Total RNA samples were collected from three biologically
467 independent replicates for each time point using the PureLink® RNA Mini Kit (Life Technology)
468 according to the manufacture's instruction. The synthesis of the first strand cDNA was carried
469 out using the Superscript III cDNA synthesis kit (Invitrogen). The real-time PCR was performed
470 using the SYBR FAST qPCR master mix (KAPA Biosystems, Wilmington, MA) on a realplex^2
471 instrument (Eppendorf). The house-keeping gene *TEF1* was used to normalize the gene
472 transcript level as we described previously (33). To examine the transcript levels of the genes of
473 our interest during unisexual mating, the wild-type XL280α, the gene deletion mutants, and the
474 gene overexpression strains in the mating type α background (OD=1) were spotted onto V8 juice
475 agar medium. Cells were collected at 0 h, 16 h, 24 h, and 48 h post inoculation. Overnight liquid
476 culture of XL280α in YPD medium was used as the reference. The extraction of total RNAs and
477 the synthesis of the first strand cDNA were carried out using the same procedures as described
478 above. The relative levels of transcripts were quantified by real-time PCR as we described
479 previously (6, 28). Primers for real-time PCR are included in the Supplemental Table 2.

Funding Statement

This work was supported by National Institutes of Health (http://www.niaid.nih.gov/Pages/default.aspx) (R01AI097599 to XL) and by China Scholarship Council (No. 201306580029 to Y. M.). Dr. Lin holds an Investigator Award in the Pathogenesis of Infectious Disease from the Burroughs Wellcome Fund (http://www.bwfund.org/)(1012445 to XL). The funders had no role in study design, data collection and interpretation, or the decision to submit the work for publication.

Author Contributions

Y.M., Y.F., and X.L. conceived and designed the experiments; Y.M. and Y.F. performed the experiments; Y.M., Y.F., and X.L. analyzed the data; X.L. contributed reagents/materials/analysis tools; Y.M., Y.F., and X.L. wrote the paper. Y.M., Y.F., W.L.and X.L. edited the paper.

Acknowledgement

We thank Lin lab members for their helpful suggestions.

References

1. Park BJ, Wannemuehler KA, Marston BJ, Govender N, Pappas PG, Chiller TM. 2009. Estimation of the current global burden of cryptococcal meningitis among persons living with HIV/AIDS. Aids 23:525-30.
2. Rajasingham R, Smith RM, Park BJ, Jarvis JN, Govender NP, Chiller TM, Denning DW, Loyse A, Boulware DR. 2017. Global burden of disease of HIV-associated cryptococcal meningitis: an updated analysis. Lancet Infect Dis 17:873-881.
3. Wang L, Lin X. 2012. Morphogenesis in Fungal Pathogenicity: Shape, Size, and Surface. PLoS Pathog 8:e1003027.
4. Sil A, Andrianopoulos A. 2014. Thermally dimorphic human fungal pathogens-polyphyletic pathogens with a convergent pathogenicity trait. Cold Spring Harb Perspect Med doi:10.1101/cshperspect.a019794.
5. Zhai B, Wozniak KL, Masso-Silva J, Upadhyay S, Hole C, Rivera A, Wormley FL, Lin X. 2015. Development of Protective Inflammation and Cell-Mediated Immunity against Cryptococcus neoformans after Exposure to Hyphal Mutants. mBio 6.
6. Wang L, Zhai B, Lin X. 2012. The link between morphotype transition and virulence in Cryptococcus neoformans. PLoS Pathog 8:e1002765.
7. Kwon-Chung KJ. 1976. Morphogenesis of Filobasidiella neoformans, the Sexual State of Cryptococcus neoformans. Mycologia 68:821-833.
8. Heitman J. 2010. Evolution of Eukaryotic Microbial Pathogens via Covert Sexual Reproduction. Cell Host & Microbe 8:86-99.
9. Idnurm A, Bahn YS, Nielsen K, Lin X, Fraser JA, Heitman J. 2005. Deciphering the model pathogenic fungus Cryptococcus neoformans. Nat Rev Microbiol 3:753-64.
10. Davidson RC, Nichols CB, Cox GM, Perfect JR, Heitman J. 2003. A MAP kinase cascade composed of cell type specific and non-specific elements controls mating and differentiation of the fungal pathogen Cryptococcus neoformans. Mol Microbiol 49:469-85.
11. Lin X, Jackson JC, Feretzaki M, Xue C, Heitman J. 2010. Transcription factors Mat2 and Znf2 operate cellular circuits orchestrating opposite- and same-sex mating in Cryptococcus neoformans. PLoS Genet 6:e1000953.
12. Zhai B, Zhu P, Foyle D, Upadhyay S, Idnurm A, Lin X. 2013. Congenic strains of the filamentous form of Cryptococcus neoformans for studies of fungal morphogenesis and virulence. Infect Immun 81:2626-37.
13. Lengeler KB, Fox DS, Fraser JA, Allen A, Forrester K, Dietrich FS, Heitman J. 2002. Mating-type locus of Cryptococcus neoformans: a step in the evolution of sex chromosomes. Eukaryot Cell 1:704-18.
14. Shen W-C, Davidson RC, Cox GM, Heitman J. 2002. Pheromones Stimulate Mating and Differentiation via Paracrine and Autocrine Signaling in Cryptococcus neoformans. Eukaryotic Cell 1:366-377.
15. Fraser JA, Diezmann S, Subaran RL, Allen A, Lengeler KB, Dietrich FS, Heitman J. 2004. Convergent Evolution of Chromosomal Sex-Determining Regions in the Animal and Fungal Kingdoms. PLoS Biology 2:e384.
16. Chung S, Karos M, Chang YC, Lukszo J, Wickes BL, Kwon-Chung KJ. 2002. Molecular analysis of CPRalpha, a MATalpha-specific pheromone receptor gene of Cryptococcus neoformans. Eukaryot Cell 1:432-9.

17. Wang L, Lin X. 2011. Mechanisms of unisexual mating in Cryptococcus neoformans. Fungal Genet Biol 48:651-60.
18. Hull CM, Davidson RC, Heitman J. 2002. Cell identity and sexual development in Cryptococcus neoformans are controlled by the mating-type-specific homeodomain protein Sxi1α. Genes & Development 16:3046-3060.
19. Schindler U, Beckmann H, Cashmore AR. 1993. HAT3.1, a novel Arabidopsis homeodomain protein containing a conserved cysteine-rich region. Plant J 4:137-50.
20. Sanchez R, Zhou M-M. 2011. The PHD finger: a versatile epigenome reader. Trends in Biochemical Sciences 36:364-372.
21. Kim J, Lee JE, Lee JS. 2015. Histone deacetylase-mediated morphological transition in Candida albicans. J Microbiol 53:805-11.
22. Dreveny I, Deeves SE, Fulton J, Yue B, Messmer M, Bhattacharya A, Collins HM, Heery DM. 2014. The double PHD finger domain of MOZ/MYST3 induces α-helical structure of the histone H3 tail to facilitate acetylation and methylation sampling and modification. Nucleic Acids Research 42:822-835.
23. Pijnappel WW, Schaft D, Roguev A, Shevchenko A, Tekotte H, Wilm M, Rigaut G, Seraphin B, Aasland R, Stewart AF. 2001. The S. cerevisiae SET3 complex includes two histone deacetylases, Hos2 and Hst1, and is a meiotic-specific repressor of the sporulation gene program. Genes Dev 15:2991-3004.
24. Hnisz D, Majer O, Frohner IE, Komnenovic V, Kuchler K. 2010. The Set3/Hos2 histone deacetylase complex attenuates cAMP/PKA signaling to regulate morphogenesis and virulence of *Candida albicans*. PLoS Pathog 6:e1000889.
25. Lin X, Huang JC, Mitchell TG, Heitman J. 2006. Virulence attributes and hyphal growth of *C. neoformans* are quantitative traits and the *MAT*alpha allele enhances filamentation. PLoS Genet 2:e187.
26. Feretzaki M, Hardison SE, Wormley FL, Jr., Heitman J. 2014. *Cryptococcus neoformans* hyperfilamentous strain is hypervirulent in a murine model of cryptococcal meningoencephalitis. PLoS One 9:e104432.
27. Ni M, Feretzaki M, Li W, Floyd-Averette A, Mieczkowski P, Dietrich FS, Heitman J. 2013. Unisexual and heterosexual meiotic reproduction generate aneuploidy and phenotypic diversity *de novo* in the yeast *Cryptococcus neoformans*. PLoS Biol 11:e1001653.
28. Wang L, Tian X, Gyawali R, Upadhyay S, Foyle D, Wang G, Cai JJ, Lin X. 2014. Morphotype transition and sexual reproduction are genetically associated in a ubiquitous environmental pathogen. PLoS Pathog 10:e1004185.
29. Zhai B, Zhu P, Foyle D, Upadhyay S, Idnurm A, Lin X. 2013. Congenic Strains of the Filamentous Form of Cryptococcus neoformans for Studies of Fungal Morphogenesis and Virulence. Infection and Immunity 81:2626-2637.
30. Gyawali R, Zhao Y, Lin J, Fan Y, Xu X, Upadhyay S, Lin X. 2017. Pheromone independent unisexual development in Cryptococcus neoformans. PLOS Genetics 13:e1006772.
31. Erke KH. 1976. Light microscopy of basidia, basidiospores, and nuclei in spores and hyphae of Filobasidiella neoformans (Cryptococcus neoformans). Journal of Bacteriology 128:445-455.
32. Kent CR, Ortiz-Bermudez P, Giles SS, Hull CM. 2008. Formulation of a defined V8 medium for induction of sexual development of Cryptococcus neoformans. Appl Environ Microbiol 74:6248-53.
33. Chacko N, Zhao Y, Yang E, Wang L, Cai JJ, Lin X. 2015. The lncRNA RZE1 Controls Cryptococcal Morphological Transition. PLoS Genet 11:e1005692.
34. Bergman A, Casadevall A. 2010. Mammalian Endothermy Optimally Restricts Fungi and Metabolic Costs. mBio 1.

35. Chen Y-L, Lehman VN, Lewit Y, Averette AF, Heitman J. 2013. Calcineurin Governs Thermotolerance and Virulence of Cryptococcus gattii. G3: Genes|Genomes|Genetics 3:527-539.
36. Walton FJ, Heitman J, Idnurm A. 2006. Conserved Elements of the RAM Signaling Pathway Establish Cell Polarity in the Basidiomycete Cryptococcus neoformans in a Divergent Fashion from Other Fungi. Molecular Biology of the Cell 17:3768-3780.
37. Magditch DA, Liu T-B, Xue C, Idnurm A. 2012. DNA Mutations Mediate Microevolution between Host-Adapted Forms of the Pathogenic Fungus Cryptococcus neoformans. PLOS Pathogens 8:e1002936.
38. Lin J, Idnurm A, Lin X. 2015. Morphology and its underlying genetic regulation impact the interaction between Cryptococcus neoformans and its hosts. Medical mycology 53:493-504.
39. Lin X. 2009. *Cryptococcus neoformans*: morphogenesis, infection, and evolution. Infect Genet Evol 9:401-16.
40. Musselman CA, Kutateladze TG. 2009. PHD Fingers: Epigenetic Effectors and Potential Drug Targets. Molecular Interventions 9:314-323.
41. Bienz M. 2006. The PHD finger, a nuclear protein-interaction domain. Trends in Biochemical Sciences 31:35-40.
42. Kwon-Chung KJ. 1975. A new genus, *Filobasidiella*, the perfect state of *Cryptococcus neoformans*. Mycologia 67:1197-200.
43. Lin X, Hull CM, Heitman J. 2005. Sexual reproduction between partners of the same mating type in *Cryptococcus neoformans*. Nature 434:1017-21.
44. Gyawali R, Upadhyay S, Way J, Lin X. 2016. Characterizing a family of secretory proteins associated with different morphotypes in Cryptococcus neoformans. Applied and Environmental Microbiology doi:10.1128/aem.02967-16.
45. Kim MS, Kim SY, Yoon JK, Lee YW, Bahn YS. 2009. An efficient gene-disruption method in *Cryptococcus neoformans* by double-joint PCR with NAT-split markers. Biochem Biophys Res Commun 390:983-8.
46. Toffaletti DL, Rude TH, Johnston SA, Durack DT, Perfect JR. 1993. Gene transfer in Cryptococcus neoformans by use of biolistic delivery of DNA. J Bacteriol 175:1405-11.
47. Lin X, Chacko N, Wang L, Pavuluri Y. submitted. Generation of stable mutants and targeted gene deletion strains in *Cryptococcus neoformans* through electroporation. Medical Mycology.
48. Lin X, Hull CM, Heitman J. 2005. Sexual reproduction between partners of the same mating type in Cryptococcus neoformans. Nature 434:1017-1021.
49. Lin X, Litvintseva AP, Nielsen K, Patel S, Floyd A, Mitchell TG, Heitman J. 2007. alpha AD alpha hybrids of *Cryptococcus neoformans*: evidence of same-sex mating in nature and hybrid fitness. PLoS Genet 3:1975-90.
50. Lin X, Patel S, Litvintseva AP, Floyd A, Mitchell TG, Heitman J. 2009. Diploids in the *Cryptococcus neoformans* serotype A population homozygous for the α mating type originate via unisexual mating. PLoS Pathog 5:e1000283 (1-18).
51. Lin X, Nielsen K, Patel S, Heitman J. 2008. Impact of Mating Type, Serotype, and Ploidy on the Virulence of Cryptococcus neoformans. Infection and Immunity 76:2923-2938.
52. Walton FJ, Idnurm A, Heitman J. 2005. Novel gene functions required for melanization of the human pathogen Cryptococcus neoformans. Molecular Microbiology 57:1381-1396.

Figure Legend

Figure 1: Multiple-sequence alignment for the 16 PHD domains and the domain structure of the PHD finger genes in *Cryptococcus neoformans*. (**A**) Multiple-sequence alignment analysis of 16 PHD domains in *Cryptococcus neoformans* showed that they share a same basic topology: two zinc atoms harbored by the Cys4-His-Cys3 motif. (**B**) The PHD finger proteins in *C. neoformans* may contain one or two PHD finger domains. Some harbor other functional domains related to chromatin modifications, such as the MOZ/SAS domain in Phd11 and the SET domain in Set302. The positions of these domains are indicated in the diagram.

Figure 2: The transcripts levels of PHD genes during yeast growth. (**A**) The transcript levels for all PHD genes are relatively low during vegetative yeast growth in YPD medium based on our RNA-seq data (33). The FPKM value of the house-keeping gene *TEF1* was used as the reference. *RUM1*α (15) was not included in the RNA-seq database due to its omission in the current genome annotation file. (**B**) The transcript level of each PHD finger gene in the wild-type strain XL280 cultured in YPD medium for 16 h was measured by real-time PCR. The transcript level of *TEF1* was used as the reference.

Figure 3. The PHD genes showed differential patterns of expression during unisexual-mating. The changes in the transcript levels of PHD genes in the wild-type strain cultured under mating-stimulating condition (V8 medium) for different time periods. The overnight culture of the wild type in YPD medium was used as the 0 time point. The transcript level of each gene at 24 h, 48 h, and 72 h after inoculation on V8 was compared to that in YPD medium. The FPKMs

of *TEF1* at the different time points were used as the reference. Two-way ANOVA multi-comparison was used for statistical analysis. The ones with statistical significance were listed below the figure. (ns: not significant with $p>0.05$; * $p \leq 0.05$; ** $p \leq 0.01$; *** $p \leq 0.001$; **** $p \leq 0.0001$)

Figure 4. The transcript levels of PHD genes during bisexual-mating. The transcript levels of each PHD gene during XL280 **a**-α bisexual mating were measured at 3 h, 10 h, 24 h, 48 h, 72 h after inoculation on V8 mating-inducing medium by real-time PCR. The transcript level of *TEF1* was used as the reference. Two-way ANOVA multi-comparison was used for statistical analysis. The transcript level of each gene at 24 h, 48 h, and 72 h post inoculation on V8 medium was compared to that in YPD medium. The ones with statistical significance were listed below. None of the data at 3 h and 10 h showed significant difference from the 0 h time point. (ns: not significant with $p>0.05$; * $p \leq 0.05$; ** $p \leq 0.01$; *** $p \leq 0.001$; **** $p \leq 0.0001$)

Figure 5. The *phd3*Δ and *phd15*Δ mutants have temperature-dependent growth defect and longer generation time. (**A**-**B**) The PHD finger gene deletion mutants and the wild type strain were cultured on YPD medium at 30°C, 37°C, and 39°C. (**C**) The cell size of the *phd3*Δ and the wild-type strains were measured microscopically and there was no statistically significant difference in cell size. (**D**) The generation time of the *phd3*Δ and the wild-type strain cultured in YPD liquid medium was examined by plotting changes in the optimal density at 600 nm against the time.

675 **Figure 6: The sensitivity of the PHD gene deletion mutants against UV radiation.** (**A-B**) The
676 wild type strain along with all PHD finger gene deletion mutants were inoculated onto YNB
677 medium and air-dried. Cells were then treated with 300 J/m^2 of UV for 0s, 3s and 5s.

678

679 **Figure 7: Mutations of the five PHD genes affect self-filamentation**. Wild type, *bye1*Δ,
680 *phd11*Δ, *set302*Δ, *rum1*αΔ, and *znf1*αΔ were cultured on V8 agar medium at 22°C for 48 h (**A**)
681 or for 96 h (**B-C**). Wild type and strains with overexpression of *BYE1*, *PHD11*, *SET302*, *RUM1*α,
682 and *ZNF1*α in the corresponding gene deletion mutant background were cultured on V8 agar
683 medium for 96 h. Upper panels showed images of the whole colonies, while the lower panels
684 showed closer up images of the edge of colonies.

685

686 **Figure 8: The transcript level of the filamentation marker *CFL1* shows good correlation**
687 **with the filamentation phenotypes of the PHD gene deletion or overexpression strains.** The
688 transcript levels of *CFL1* were measured by real-time PCR in the wild type, the five PHD gene
689 deletion mutants (*bye1*Δ, *phd11*Δ, *set302*Δ, *rum1*αΔ, and *znf1*αΔ), and overexpression strains
690 (*BYE1*^{oe}/*bye1*Δ, *PHD11* ^{oe}/*phd11*Δ, and *SET302* ^{oe}/*set302*Δ). Overnight cultures of these strains
691 in YPD liquid medium were considered as the 0 time point. Cells were then cultured on V8 agar
692 medium for 16 h and 24 h. The *CFL1* transcript level in the wild type at the 0 time point was
693 used for normalization. The Y axis shows the Log2 changes in the transcript level of *CFL1*.

694

695 **Figure 9: Phd11 functions upstream of the master morphogenesis regulator Znf2.** (**A**) WT,
696 *znf2*Δ, and *ZNF2*^{oe} cells were cultured in YPD liquid medium overnight or on V8 agar medium

for 24 h . The transcript levels of *PHD11* were measured by real-time PCR. The *PHD11* transcript level in WT cultured in YPD medium was used as the reference. (**B**) WT, *phd11*Δ, and *PHD11*^{oe} cells were cultured in YPD liquid medium overnight or on V8 medium for 16 h. The transcript levels of *ZNF2* were measured by RT-PCR. The *ZNF2* transcript level of WT cultured in YPD was used as the reference. (**C**) WT, *phd11*Δ, *znf2*Δ, and *phd11*Δ*znf2*Δ double mutant were cultured on V8 agar medium for 3 days. (**D**) Diagram of the strain with constitutive expression of *PHD11* driven by the *GPD1* promoter and the inducible expression of *ZNF2* driven by the *CTR4* promoter. The expression of *ZNF2* is induced by copper limitation and suppressed by excessive copper. (**E**) WT, the P$_{GPD1}$-*PHD11*/*phd11*Δ strain, the P$_{CTR4}$-*ZNF2*/*znf2*Δ strain, and the P$_{GPD1}$-*PHD11*/P$_{CTR4}$-*ZNF2*/*znf2*Δ strain were cultured on copper limited V8 juice agar medium (*ZNF2*-inducing condition) and on V8 agar supplemented with 50μM $CuSO_4$ (*ZNF2*-suppressing condition).

Figure 10: Phd11 is located in the nucleus. The Phd11-mCherry strain was cultured in YPD medium. Cells were fixed and stained with DAPI.

712 **Table 1. 15 PHD genes encoded in the genomes of JEC21 and H99**

Gene Name	Gene ID in JEC21	Gene ID in H99	Homologue in *S.c*
PHD1	CNG02500	CNAG_03329	Pho23 in *Sc*
BYE1	CNK01990	CNAG_01859	Bye1 in *Sc*
PHD3	CNK01390	CNAG_07532	Yng1 in *Sc*
PHD4	CNK00900	CNAG_02604	
PHD5	CNI02340	CNAG_04315	
PHD6	CNG01620	CNAG_03423	
PHD7	CNG01970	CNAG_03388	
SPP101(PHD8)	CNG01770	CNAG_03406	Spp1 in *Sc*
PHD9	CNC00260	CNAG_07967	
PHD11	CNG00240	CNAG_03583	
SET302(PHD12)	CNF04280	CNAG_06591	Set3 in *Sc*
RUM1(PHD13)	CND05870	CNAG_07411	
ZNF1(PHD14)	CND05730	[a]	
PHD15	CND04210	CNAG_01301	Yng2 in *Sc*
PHD16	CND03810	CNAG_07430	Cti6 in *Sc*

713 [a] *ZNF1* exists in H99 (13) but there is no annotation of this gene in the current genome database.

Table 2. Strains and plasmid used in this study

Strains	Genotype	Source
XL280α	wild type	(48)
XL280**a**	wild type	(12)
YM1	MAT alpha,*PHD1*::G418	This study
YM3	MAT a, *PHD1*::G418	This study
YM8	MAT alpha,*BYE1*::G418	This study
YM10	MAT alpha,*PHD3*::G418	This study
YM12	MAT a, *PHD3*::G418	This study
YM20	MAT alpha *PHD4*::G418	This study
YM23	MAT a *PHD4*::G418	This study
YM27	MAT alpha *PHD5*::G418	This study
YM28	MAT a *PHD5*::G418	This study
YM32	MAT alpha *PHD6*::G418	This study
YM34	MAT alpha *PHD7*::G418	This study
YM38	MAT a, *PHD7*::G418	This study
YM42	MAT alpha, *PHD8*::G418	This study
YM45	MAT a, *PHD8*::G418	This study
YM66	MAT alpha, *PHD9*::NAT	This study
YM50	MAT alpha, *PHD11*::NAT	This study
YM52	MAT a, *PHD11*::NAT	This study
YM60	MAT alpha, *SET302*::NAT	This study
YF36	MAT a, *SET302*::NAT	This study
YM61	MAT alpha, *RUM1*::NAT	This study
YF92	MAT a,*RUM1*::NAT	This study
XL571	MAT alpha, *ZNF1*::NAT	(11)
YM69	MAT a, *ZNF1*::NAT	This study
YM62	MAT alpha, *PHD15*::NAT	This study
YF63	MAT a, *PHD15*::NAT	This study
YM63	MAT alpha, *PHD16*::NAT	This study
YM64	MAT a, *PHD16*::NAT	This study
YM72	MAT alpha, P_{GPD1}-*PHD11*-mCherry::NEO	This study
YF58	MAT alpha, P_{GPD1}-*SET302*-HYG, *SET302*::NAT	This study
YF27	MAT alpha, *RUM1*::NAT, P_{GPD1}-*RUM1*-HYG	This study
YF30	MAT alpha, *ZNF1*::NAT, P_{GPD1}-*ZNF1*-HYG	This study
YF159	MAT alpha, P_{GPD1}-BYE1-HYG, *BYE1*::NEO	This study
XL574	MAT alpha, *ZNF2*::NAT	(11)
YF133	MAT alpha, *PHD11*::NAT, *ZNF2*::NAT	This study
XX17	MAT alpha, *ZNF2*::NAT, P_{CTR4}-mcherry-*ZNF2* (G418)	(33)
LW1	MAT alpha, *ZNF2*::NAT, P_{GPD1}-*ZNF2*D-NEO	(6)

Strains	Genotype	Source
YF127	MAT alpha, P_{GPD1}-*PHD11*-HYG, *ZNF2*::NAT, pCTR4-mcherry-*ZNF2* (G418)	This study
XL1348	MAT alpha, XL280α $G418^r$	This study
XL1109	MAT alpha, XL280α NAT^r	This study
XL1142	MAT a, JEC20**a** NAT^r	This study
XL1411	MAT a, JEC20**a** $G418^r$	This study
XL942	MAT alpha, *MAT2*::NAT	(11)

plasmid	Genotype	Source
pXL1-PHD11-mcherry	p_{GPD1}-*PHD11*-mCherry-G418	This Study
pXL1-SET302	P_{GPD1}-*SET302*-HYG	This Study
pXL1-RUM1	P_{GPD1}-*RUM1*-HYG	This Study
pXL1-ZNF1	P_{GPD1}-*ZNF1*-HYG	This Study
pXL1-PHD11	P_{GPD1}-*PHD11*-HYG	This Study
pXL1-BYE1	PGPD1-BYE1-HYG	This Study
pPZP-NEO1	pPZP-NEO1	(52)
pPZP-NATcc	pPZP-NATcc	(52)

714

Table 3: Primers used in this study

Primer#	Name	Sequence
	M13F	GTAAAACGACGGCCAG
	M13R	AACAGCTATGACCATG
Linlab2091	PHD1-Left Forward	CTACATGTGACACTTACCGTACTG
Linlab2092	PHD1-M13F complement+Left Reverse	CTGGCCGTCGTTTTACCTGGTAGATGAGCGCTATG
Linlab2093	PHD1-M13R complement+Right Forward	GTCATAGCTGTTTCCTGCCTATCCATACCCCTTATAATG
Linlab2094	PHD1-Right Reverse	AAGAATTGGAGGATTTACAAAG
Linlab2095	PHD1-Far left forward	TCGTCTCGAGAGGTAGTTGTC
Linlab2096	BYE1-Left Forward	ACATGCAGCTTTGTGATACG
Linlab2097	BYE1-M13F complement+Left Reverse	CTGGCCGTCGTTTTACAAGCTGTGTCTATCCCGC
Linlab2098	BYE1-M13R complement+Right Forward	GTCATAGCTGTTTCCTGGTATTGTTGCACGTGTTCAGTC
Linlab2099	BYE1-Right Reverse	AGCGCTGTTATTTCTTATCG
Linlab2100	BYE1-Far left forward	ATGCGACTCCACCACTACTAG
Linlab2288	BYE1-Left-forward-nested	CATGGCTTTGTTGCTTCAC
Linlab2101	PHD3-Left Forward	CACGAAAGTATCTTCATTCATTG
Linlab2102	PHD3-M13F complement+Left Reverse	CTGGCCGTCGTTTTACTGTAGGGCGAATTATATGG
Linlab2103	PHD3-M13R complement+Right Forward	GTCATAGCTGTTTCCTGTACTATCGTTACTGGCACATAC
Linlab2104	PHD3-Right Reverse	GAAACTCACTGCCGTAGAGG
Linlab2105	PHD3-Far left forward	GCTACCTCTTTGTCTACTACTGC
Linlab2106	PHD4-Left Forward	CCTATCGATGGAGTAGAGCC
Linlab2107	PHD4-M13F complement+Left Reverse	CTGGCCGTCGTTTTACATTCATGCCCTCGGAGC
Linlab2108	PHD4-M13R complement+Right Forward	GTCATAGCTGTTTCCTGATCCTGCCTTTCTCAATGC
Linlab2109	PHD4-Right Reverse	CATCCATCACACTGCATACTC
Linlab2110	PHD4-Far left forward	GCATCCAGGACAATTACATC
Linlab2225	PHD4-Right reverse2	CGCCTTTCATGACTCTCG
Linlab2289	PHD4-Left-forward-nested	TGTTCAGCCCTTCTCGTG
Linlab2160	PHD5-Left Forward	GGACGAGAGAGAGGACGAG
Linlab2161	PHD5-M13F complement+Left Reverse	CTGGCCGTCGTTTTACAGATGCACCGATGAGCG
Linlab2162	PHD5-M13R complement+Right Forward	GTCATAGCTGTTTCCTGCCATCGGCGTTTGACTG
Linlab2163	PHD5-Right Reverse	ATCCGAGCTGTCGTTGG
Linlab2164	PHD5-Far left forward	CCATCACCTCCGAGCT
Linlab2165	PHD6-Left Forward	AGCAACGCTGGATCTGG
Linlab2166	PHD6-M13F complement+Left Reverse	CTGGCCGTCGTTTTACATACAGCGATGGAAAGTGG
Linlab2167	PHD6-M13R complement+Right Forward	GTCATAGCTGTTTCCTGGTGCATAGGCATATACTTGG
Linlab2168	PHD6-Right Reverse	GGTACCGCCTGCACAAG
Linlab2169	PHD6-Far left forward	TGGAGGTCCTCGAACTCTG
Linlab2348	PHD6-Left Forward-nested	GGCGACAACAGTTGCATAG
Linlab2349	PHD6-Right reverse-nested	TCAGCAGACTCAATCAGCG

Linlab2170	PHD7-Left Forward	AAACGGTATTGATCTTCGC
Linlab2171	PHD7-M13F complement+Left Reverse	CTGGCCGTCGTTTTACACTGATGCGATGTTATGCC
Linlab2172	PHD7-M13R complement+Right Forward	GTCATAGCTGTTTCCTGCGTTCACCGAACTGTACG
Linlab2173	PHD7-Right Reverse	CTGTTGTTGCCAACCCTG
Linlab2174	PHD7-Far left forward	AGAGCCGCTGAGTCCTTC
Linlab2175	PHD8-Left Forward	CGGTCATGGCGTAGAGTC
Linlab2176	PHD8-M13F complement+Left Reverse	CTGGCCGTCGTTTTACAAGACAAGGGCAAAGCG
Linlab2177	PHD8-M13R complement+Right Forward	GTCATAGCTGTTTCCTGGCATGTGCATCTCCTCTCC
Linlab2178	PHD8-Right Reverse	CCCAGAGCCATCTAGCG
Linlab2179	PHD8-Far left forward	AGGCGACTTTCGTGATTG
Linlab2356	PHD9-Left forward-nested	GGCTGCGAAGGACAAAG
Linlab2357	PHD9-Right reverse-nested	TGGCTTCCTGTCACTTGC
Linlab2220	PHD9-Left Forward	CACGAGCACTTGGATGG
Linlab2221	PHD9-M13F complement+Left Reverse	CTGGCCGTCGTTTTACATTGACAACAGGTGGATGC
Linlab2222	PHD9-M13R complement+Right Forward	GTCATAGCTGTTTCCTGCCTCCAGATCCGAGATTG
Linlab2223	PHD9-Right Reverse	AGTTCACTGGGGTGTTGC
Linlab2224	PHD9-Far left forward	GCGAGGAATTTGAACCAG
Linlab2190	PHD11-Left Forward	CATCAAACTCTGCCACAGG
Linlab2191	PHD11-M13F complement+Left Reverse	CTGGCCGTCGTTTTACCGTGTCTCATGCATGGAG
Linlab2192	PHD11-M13R complement+Right Forward	GTCATAGCTGTTTCCTGCAAGTTTCGGGCTTTGG
Linlab2193	PHD11-Right Reverse	GTGGACCGAGGCGAAAG
Linlab2194	PHD11-Far left forward	GGCCGTGAAGCGTGTAG
Linlab2195	SET302-Left Forward	GGTCCGACATTTTCCAGG
Linlab2196	SET302-M13F complement+Left Reverse	CTGGCCGTCGTTTTACATCTACAAGCGGGTCAGG
Linlab2197	SET302-M13R complement+Right Forward	GTCATAGCTGTTTCCTGGCGTTACCGTTGTTGTCC
Linlab2198	SET302-Right Reverse	CCCCTTTTCGCTTTTGC
Linlab2199	SET302-Far left forward	AAGCGTTGGGATCCCAG
Linlab2350	SET302-Left forward-nested	CTCGCTTTCGGGATGAG
Linlab2351	SET302-Right reverse-nested	CAACGGCTTAACCCTGTC
Linlab2200	RUM1-Left Forward	GCCACAACTCGTCCGTG
Linlab2201	RUM1-M13F complement+Left Reverse	CTGGCCGTCGTTTTACAAAGGGAGTGCGTGCTG
Linlab2202	RUM1-M13R complement+Right Forward	GTCATAGCTGTTTCCTGCCTTCCAGATTCGTGAGC
Linlab2203	RUM1-Right Reverse	GAGCTGCTCGATGTACCAC
Linlab2204	RUM1-Far left forward	CGTCACCATCATTTCCG
Linlab2205	ZNF1-Left Forward	AACTCCTGGGCTCAACG
Linlab2206	ZNF1-M13F complement+Left Reverse	CTGGCCGTCGTTTTACTTTGCACAGGGTGACCAG
Linlab2207	ZNF1-M13R complement+Right Forward	GTCATAGCTGTTTCCTGATTCCGGCTGATGCTTC
Linlab2208	ZNF1-Right Reverse	CCAAGCTTGGCAATTCG
Linlab2209	ZNF1-Far left forward	GCAAGCGTTGGCTCAAC

Linlab2210	PHD15-Left Forward	TGTGAAGCCGAGGGACC
Linlab2211	PHD15-M13F complement+Left Reverse	CTGGCCGTCGTTTTACAGATGGATGAGTGGCGG
Linlab2212	PHD15-M13R complement+Right Forward	GTCATAGCTGTTTCCTGGCGAGATGGTTGCTTTTG
Linlab2213	PHD15-Right Reverse	TCCAACCTCCAACACCAC
Linlab2214	PHD15-Far left forward	GCTTCCGGGGATAAACC
Linlab2352	PHD15-Left forward-nested	TGGCTAGAGGAATGGCTG
Linlab2353	PHD15-Right reverse-nested	TGTGTTTTGCGGTGTTGAG
Linlab2354	PHD16-Left forward-nested	CACCGAGTACAGCTGCAAC
Linlab2355	PHD16-Right reverse-nested	GGCGTTCAGACTCCTTTG
Linlab2176	PHD8-M13F complement+Left Reverse	CTGGCCGTCGTTTTACAAGACAAGGGCAAAGCG
Linlab2177	PHD8-M13R complement+Right Forward	GTCATAGCTGTTTCCTGGCATGTGCATCTCCTCTCC
Linlab2178	PHD8-Right Reverse	CCCAGAGCCATCTAGCG
Linlab2179	PHD8-Far left forward	AGGCGACTTTCGTGATTG
Linlab2356	PHD9-Left forward-nested	GGCTGCGAAGGACAAAG
Linlab2357	PHD9-Right reverse-nested	TGGCTTCCTGTCACTTGC
Primer#	Name	Sequence
Linlab2220	PHD9-Left Forward	CACGAGCACTTGGATGG
Linlab2221	PHD9-M13F complement+Left Reverse	CTGGCCGTCGTTTTACATTGACAACAGGTGGATGC
Linlab2222	PHD9-M13R complement+Right Forward	GTCATAGCTGTTTCCTGCCTCCAGATCCGAGATTG
Linlab2223	PHD9-Right Reverse	AGTTCACTGGGGTGTTGC
Linlab2224	PHD9-Far left forward	GCGAGGAATTTGAACCAG
Linlab2190	PHD11-Left Forward	CATCAAACTCTGCCACAGG
Linlab2191	PHD11-M13F complement+Left Reverse	CTGGCCGTCGTTTTACCGTGTCTCATGCATGGAG
Linlab2192	PHD11-M13R complement+Right Forward	GTCATAGCTGTTTCCTGCAAGTTTCGGGCTTTGG
Linlab2193	PHD11-Right Reverse	GTGGACCGAGGCGAAAG
Linlab2194	PHD11-Far left forward	GGCCGTGAAGCGTGTAG
Linlab2195	SET302-Left Forward	GGTCCGACATTTTCCAGG
Linlab2196	SET302-M13F complement+Left Reverse	CTGGCCGTCGTTTTACATCTACAAGCGGGTCAGG
Linlab2197	SET302-M13R complement+Right Forward	GTCATAGCTGTTTCCTGGCGTTACCGTTGTTGTCC
Linlab2198	SET302-Right Reverse	CCCCTTTTCGCTTTTGC
Linlab2199	SET302-Far left forward	AAGCGTTGGGATCCCAG
Linlab2350	SET302-Left forward-nested	CTCGCTTTCGGGATGAG
Linlab2351	SET302-Right reverse-nested	CAACGGCTTAACCCTGTC
Linlab2200	RUM1-Left Forward	GCCACAACTCGTCCGTG
Linlab2201	RUM1-M13F complement+Left Reverse	CTGGCCGTCGTTTTACAAAGGGAGTGCGTGCTG
Linlab2202	RUM1-M13R complement+Right Forward	GTCATAGCTGTTTCCTGCCTTCCAGATTCGTGAGC
Linlab2203	RUM1-Right Reverse	GAGCTGCTCGATGTACCAC
Linlab2204	RUM1-Far left forward	CGTCACCATCATTTCCG

Linlab2205	ZNF1-Left Forward	AACTCCTGGGCTCAACG
Linlab2206	ZNF1-M13F complement+Left Reverse	CTGGCCGTCGTTTTACTTTGCACAGGGTGACCAG
Linlab2208	ZNF1-Right Reverse	CCAAGCTTGGCAATTCG
Linlab2207	ZNF1-M13R complement+Right Forward	GTCATAGCTGTTTCCTGATTCCGGCTGATGCTTC
Linlab2209	ZNF1-Far left forward	GCAAGCGTTGGCTCAAC
Linlab2210	PHD15-Left Forward	TGTGAAGCCGAGGGACC
Linlab2211	PHD15-M13F complement+Left Reverse	CTGGCCGTCGTTTTACAGATGGATGAGTGGCGG
Linlab2212	PHD15-M13R complement+Right Forward	GTCATAGCTGTTTCCTGGCGAGATGGTTGCTTTTG
Linlab2213	PHD15-Right Reverse	TCCAACCTCCAACACCAC
Linlab2214	PHD15-Far left forward	GCTTCCGGGGATAAACC
Linlab2352	PHD15-Left forward-nested	TGGCTAGAGGAATGGCTG
Linlab2353	PHD15-Right reverse-nested	TGTGTTTTGCGGTGTTGAG
Linlab2354	PHD16-Left forward-nested	CACCGAGTACAGCTGCAAC
Linlab2355	PHD16-Right reverse-nested	GGCGTTCAGACTCCTTTG
Linlab2215	PHD16-Left Forward	CGATGCTGATTTACCCG
Linlab2216	PHD16-M13F complement+Left Reverse	CTGGCCGTCGTTTTACTGGATGAAGAGTTGCTCG
Linlab2217	PHD16-M13Rcomplement+RightForward	GTCATAGCTGTTTCCTGCGGGATATCGGGTGTTC
Linlab2218	PHD16-Right Reverse	AGCCTCGGACGATCCTG
Linlab2219	PHD16-Far left forward	GTCTTGGAAGCAACCTCG
Linlab2669	Fse1+PHD11 Left Forward	TGATCTGGCCGGCCGACAGAATCAAACTCTCCATGC
Linlab2724	Asisi+PHD11 Right Reverse	ATATGCGATCGCAACATCATAGTCAATATACTCCTCATC
Linlab3279	Pac1+PHD11Right Reverse	GTTTAATTAATCAAACATCATAGTCAATATACTCC
Linlab2828	FseI+BYE1-LeftForward	TGATCTGGCCGGCCATGGCAGGTCCAGTCATC
Linlab3219	PacI+BYE1-Right Reverse	GTTTAATTAACTATTCCTCCTCCTTTTCTTC
Linlab2901	Fse1+SET302-Left Forward	TGATCTGGCCGGCCAAATGGACACCATCAACC
Linlab3220	PacI+SET302-Right Reverse	GTTTAATTAATTATCCACCTCTCCCACG
Linlab2903	Fse1+RUM1+Left Forward	TGATCTGGCCGGCCAATGCTGCCATCAAGCC
Linlab3137	PacI+RUM1+ Right Reverse	GTTTAATTAATTATTGGTTCTCCATAGTAACATC
Linlab2949	Fse1+ZNF1+Left Forward	TGATCTGGCCGGCCATGTGTATGTTTCACTACCTTG
Linlab3138	PacI+ZNF1+Right Reverse	GTTTAATTAACTAATTTTGGTTCTTAAAC
Linlab2405	PHD1-RT-left forward	GCAAGGTGGAAGAAAACTG
Linlab2406	PHD1-RT-right reverse	CGTTATCACAGCCAATCATC
Linlab2787	PHD2-RT-left forward	CCTCGATGGCCTAGTCTAC
Linlab2788	PHD2-RT-right reverse	GAACTCGACCGGATACTACTC
Linlab2407	PHD3-RT-left forward	GTATGCCGAGATGGAGATG
Linlab2408	PHD3-RT-right reverse	TCTTTCGCCTCTCAATACAC
Linlab2789	PHD4-RT-left forward	AGAAAGGGAGCTTTTCGAG
Linlab2790	PHD4-RT-right reverse	CAGCGTCATAAGTTACCAATC
Linlab2791	PHD5-RT-left forward	CTGAAGCTGCCGTCTCTG

Linlab2792	PHD5-RT-right reverse	CTTCTTGCCTGACCCTTG
Linlab2793	PHD6-RT-left forward	CAGAATCGTCAGCAAGAGC
Linlab2794	PHD6-RT-right reverse	CGTTTCCATCCTCCATTG
Linlab2795	PHD7-RT-left forward	GATGCGCAAGAGGTCGT
Linlab2796	PHD7-RT-right reverse	TGTACGTGAGTGAATTTGAGTG
Linlab2629	PHD8-RT-left forward	TGGGAAGCTAGCCTGATC
Linlab2630	PHD8-RT-right-reverse	ATTCTCCTGCAGGCTTTC
Linlab2805	PHD9-RT-left forward	CACTGCTAGATACCCACACC
Linlab2806	PHD9-RT-right reverse	CTGCTGACGAGTGTCTTGC
Linlab2409	PHD11-RT-left forward	ACCTGTCAAGCCTGTTACC
Linlab2410	PHD11-RT-right reverse	CTCCTTCTGCATCGTCATC
Linlab2797	SET302 RT-left forward	CGTTTAGTGGTTCGGGAG
Linlab2798	SET302-RT-right reverse	TCCTCTTGACAATCCCAGAC
Linlab2799	RUM1-RT-left forward	GATTCACGTGAAGGCTCTG
Linlab2800	RUM1-RT-right reverse	CTCCATAGTAACATCTTCATCG
Linlab2821	ZNF1-RT-left forward	CGACGGAACCGTACAATC
Linlab2822	ZNF1-RT-Right reverse	GGCAGAGCAGTCGCAAT
Linlab2801	PHD15-RT-left forward	CACGTCAAATGTGTCAACATC
Linlab2802	PHD15-RT-right reverse	GTTGCCCTTGTCATTTGAG
Linlab2803	PHD16-RT-left forward	CAGGTAAGGGATTGGACG
Linlab2804	PHD16-RT-right reverse	CCTGAGTGATTTCCTCTACCT
Linlab1345	ZNF2-RT-Left Forward	GCCATCTTACCCCTACCATCTAC
Linlab1346	ZNF2-RT-Right Reverse	TGGACATAGGAACGCTGACAAT
Linlab329	TEF1-RT-Left forward	CGTCACCACTGAAGTCAAGT
Linlab330	TEF1-RT-Right Reverse	AGAAGCAGCCTCCATAGG
Linlab1341	CFL1-RT- Left forward	CTCCACTCTCGTGCTCCTGAA
Linlab1342	CFL1-RT-Right Reverse	AGTTCGCTTGCCTTTTCCTTT
Linlab1267	MFα-RT-Left Forward	ATCTTCACCACCTTCACTTCT
Linlab1268	MFα-RT-Right Reverse	CTAGGCGATGACACAAAGG

715

A

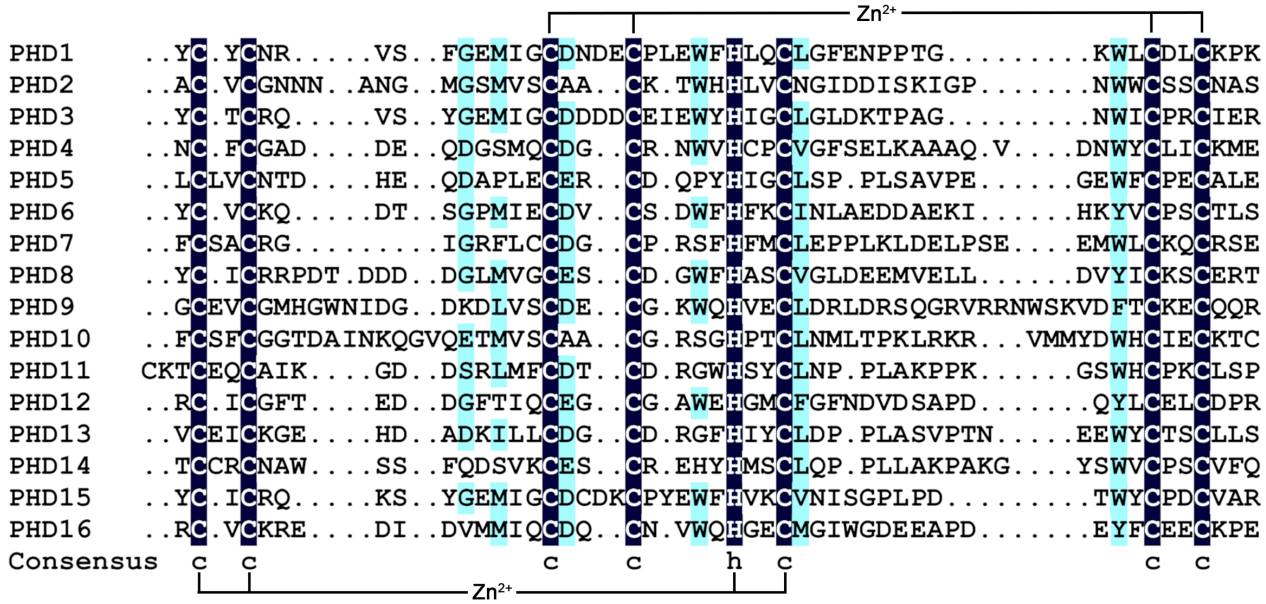

B

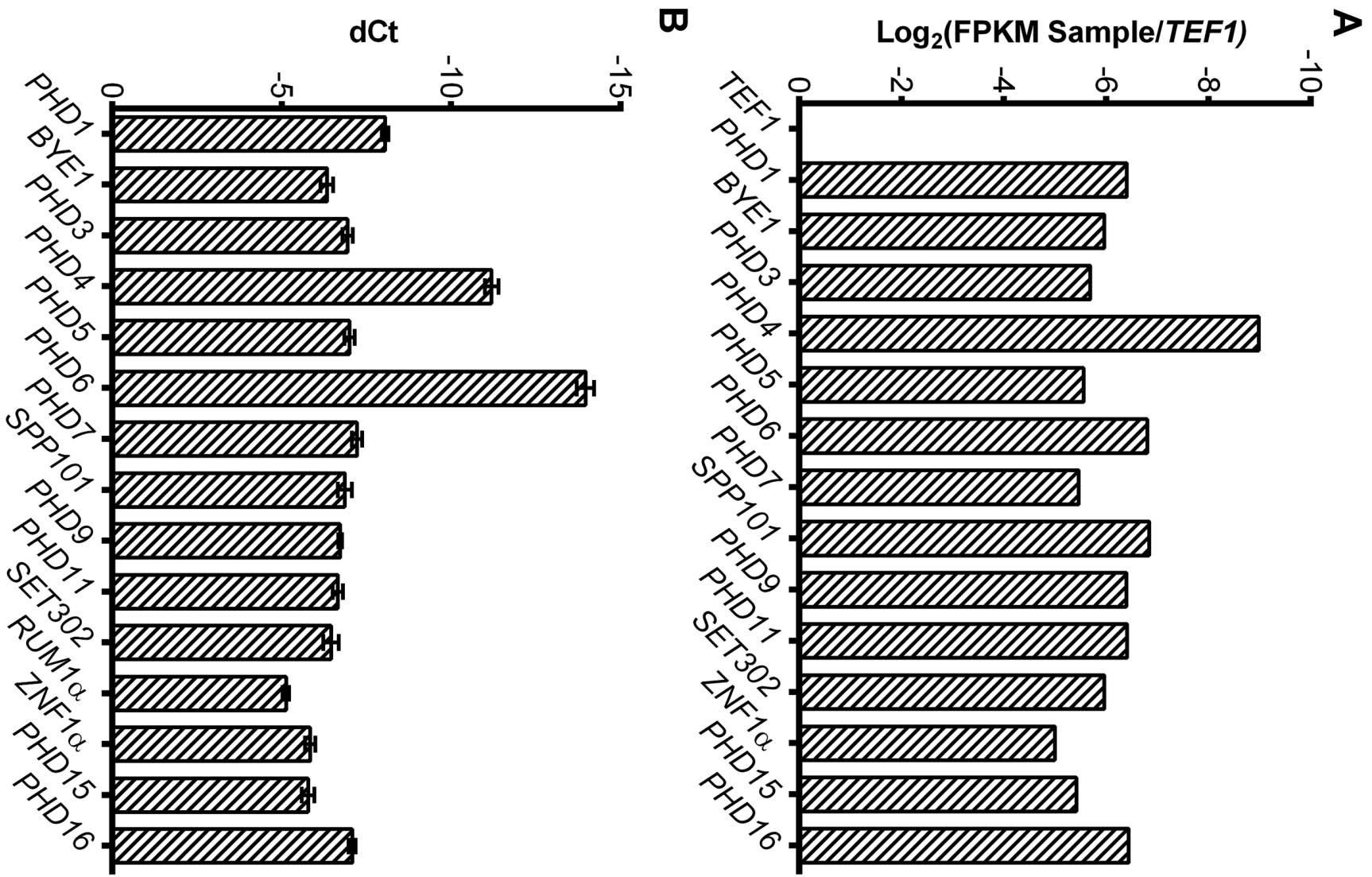

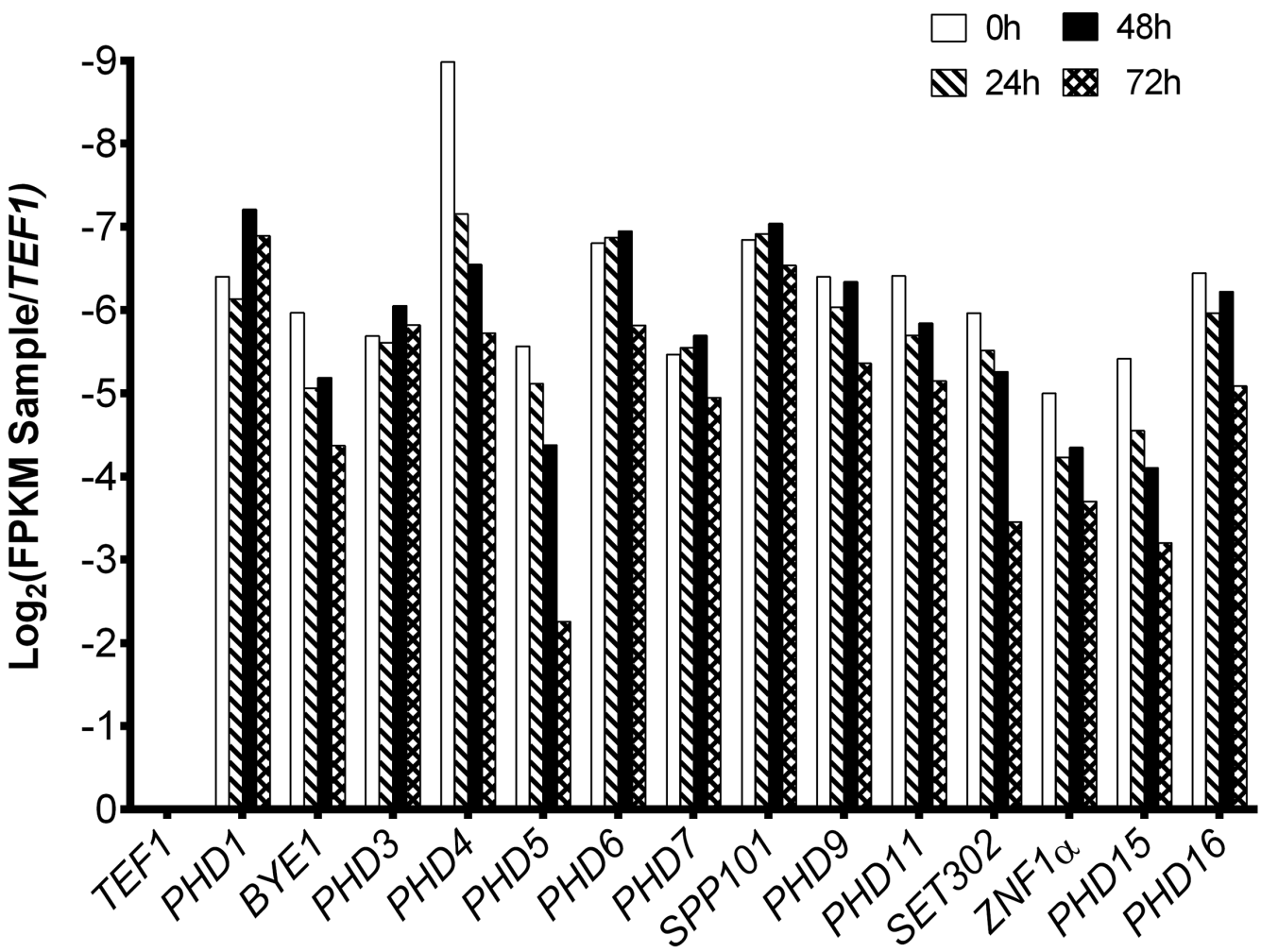

	PHD1	*BYE1*	*PHD3*	*PHD4*	*PHD5*	*PHD6*	*PHD7*
0h vs 24h	ns	**	ns	****	ns	ns	ns
0h vs 48h	**	**	ns	****	****	ns	ns
0h vs 72h	ns	****	ns	****	****	***	ns
	SPP101	*PHD9*	*PHD11*	*SET302*	*ZNF1α*	*PHD15*	*PHD16*
0h vs 24h	ns	ns	*	ns	**	**	ns
0h vs 48h	ns	ns	ns	*	*	****	ns
0h vs 72h	ns	***	****	****	****	****	ns

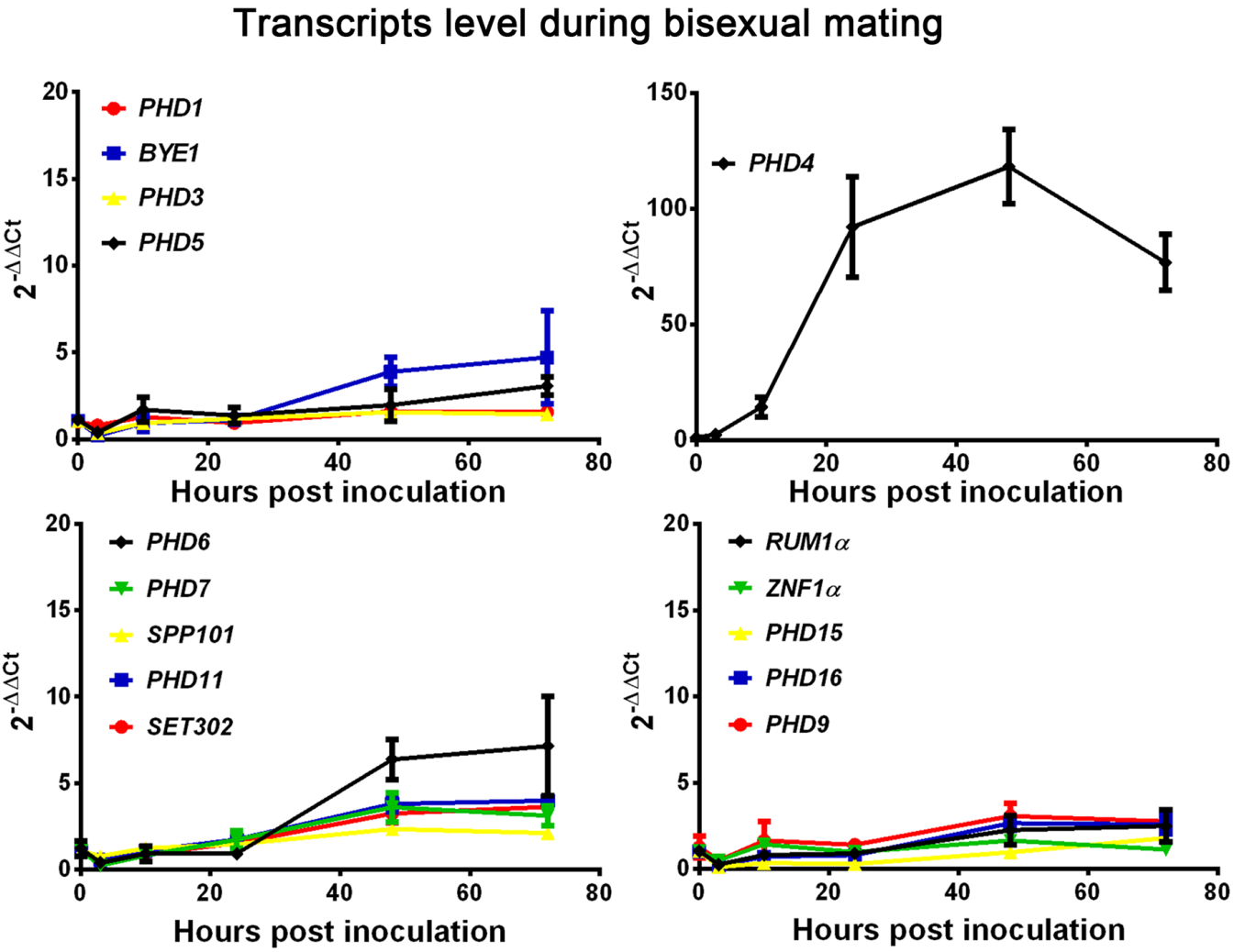

	PHD1	*BYE1*	*PHD3*	*PHD4*	*PHD5*	*PHD6*	*PHD7*	*SPP101*
0h vs 24h	ns	ns	ns	****	ns	ns	ns	ns
0h vs 48h	ns	*	ns	****	ns	****	*	ns
0h vs 72h	ns	**	ns	****	ns	****	ns	ns
	PHD9	*PHD11*	*SET302*	*RUM1α*	*ZNF1α*	*PHD15*	*PHD16*	
0h vs 24h	ns	ns	ns	ns	ns	ns	ns	
0h vs 48h	*	*	ns	ns	ns	ns	*	
0h vs 72h	ns	**	*	ns	ns	ns	**